Materials Science & Engineering A 635 (2015) 133–142

Contents lists available at ScienceDirect

Materials Science & Engineering A

journal homepage: www.elsevier.com/locate/msea

Micromechanics of twinning in a TWIP steel

K.M. Rahman [a,*], N.G. Jones [b], D. Dye [a]

[a] Department of Materials, Royal School of Mines, Imperial College London, Prince Consort Road, London SW7 2BP, UK
[b] Department of Materials Science and Metallurgy, University of Cambridge, 27 Charles Babbage Road, Cambridge CB3 0FS, UK

ARTICLE INFO

Article history:
Received 4 February 2015
Received in revised form
19 March 2015
Accepted 20 March 2015
Available online 28 March 2015

Keywords:
Twinning
Synchrotron radiation
Austenitic steel
Yield phenomena
Micromechanical modeling

ABSTRACT

The deformation behaviour of a TWinning Induced Plasticity (TWIP) steel was studied at quasi-static strain rates using synchrotron X-ray diffraction. A {111} RD and {200} RD texture developed from the earliest stages of deformation, which could be reproduced using an elasto-plastic self consistent (EPSC) model. Evidence is found from multiple sources to suggest that twinning was occurring before macroscopic yielding. This included small deviations in the lattice strains, {111} intensity changes and peak width broadening all occurring below the macroscopic yield point. The accumulation of permanent deformation on sub-yield mechanical cycling of the material was found, which further supports the diffraction data. TEM revealed that fine deformation twins similar to those observed in heavily deformed samples formed during sub-yield cycling. It is concluded that twinning had occurred before macroscopic plastic deformation began, unlike the behaviour traditionally expected from hexagonal metals such as Mg.

1. Introduction

High manganese content steels deform through the evolution of mechanical twins, and have therefore become known as TWinning Induced Plasticity (TWIP) steels. These austenitic steels are generally based on the Fe–Mn–Si–Al–C system, where the composition is adjusted to tailor the stacking fault energy (SFE) to be within a desired range [1]. Manganese and aluminium additions raise the SFE, while the addition of silicon in sufficient amounts acts to reduce the SFE [5,6]. TWIP steels exhibit extremely high strain to failure, up to 95%, at tensile strengths in excess of 800 MPa [1–3]. This extraordinary combination of properties has led to significant interest in using these steels in high strain rate energy adsorption applications, such as automotive crash safety systems and military vehicle armour [7].

The SFE is affected by temperature and composition, consequently the value is of great practical importance in face centred cubic (*fcc*) materials, particularly austenitic steels. The SFE influences the processes of dislocation cross-slip and climb [4], which have an important role in the work hardening behaviour of a material. Low SFE results in stacking faults becoming wider, thus making dislocation cross-slip more difficult. Therefore it is essential to tailor the alloy composition for a desired SFE range.

Austenitic steels deform *via* a phase transformation, mechanical twinning or dislocation glide depending on the SFE [8]. At high energies ($\geq 45\ \mathrm{mJ\,m^{-2}}$) deformation progresses solely by dislocation glide. Lower SFE ($\leq 18\ \mathrm{mJ\,m^{-2}}$) promotes a martensitic transformation to ϵ-martensite, $\gamma_{fcc} \rightarrow \epsilon_{hcp}$, which becomes a two step transformation to form α'-martensite at even lower energies, $\gamma_{fcc} \rightarrow \epsilon_{hcp} \rightarrow \alpha'_{bcc}$ [9]. A SFE ranging between 18 and $45\ \mathrm{mJ\,m^{-2}}$ promotes the formation of mechanical twins during deformation, which enables excellent ductility to be achieved.

Deformation twinning is a process which proceeds through a dislocation mechanism. Mahajan [10] proposed two salient features of deformation twin formation in *fcc* crystals; firstly a three layer twin may nucleate when two co-planar $\frac{1}{2}\langle 110\rangle$ dislocations interact, and secondly a macroscopic twin may evolve when three layer twins at different levels grow into each other. Two co-planar perfect $\frac{1}{2}\langle 110\rangle$ dislocations can react either through co-planar slip or cross glide, thus the reaction; $\frac{1}{2}[\bar{1}01]+\frac{1}{2}[\bar{1}10]\rightarrow 3\times\frac{1}{6}[\bar{2}11]$, is possible. It is believed that this reaction governs the nucleation of twins in *fcc* crystals. Furthermore in low stacking fault energy materials that twin more readily, the perfect dislocations will dissociate into Shockley partials; $\frac{1}{2}[\bar{1}10]\rightarrow\frac{1}{6}[\bar{2}11]+\frac{1}{6}[\bar{1}2\bar{1}]$. This is believed to be an intermediate step to the previous reaction as it is energetically favourable. Consequently a macroscopic twin forms when the nucleated twins grow into each other, *i.e.* absorb more partials. This may explain why twinning is less favourable in materials with high stacking fault energies, because the partials are more tightly bound *i.e.* the partial dislocation pair have a narrow core width and lower mobility. The self-thickening of twins has recently been observed *in situ* in coarse grained Cu–Ge alloys and nanocrystalline Ni [11,12]. A perfect dislocation was found to dissociate into leading and trailing partials. The leading

* Corresponding author. Tel.: +44 20 7594 6811.
E-mail address: khandaker.rahman05@imperial.ac.uk (K.M. Rahman).

http://dx.doi.org/10.1016/j.msea.2015.03.082
0921-5093/

partial subsequently splits further into a perfect dislocation and twinning partial upon encountering an obstacle. Subsequently the perfect dislocation can cross-slip and dissociate once again. This cycle continues, thereby thickening the twin on successive primary slip and cross-slip planes, without the need for the nucleation of additional Shockley partials.

Twins are observed by the formation of discrete sheared grain subregions characterised by a mirror plane at the twin interface. Consequently, the high strength and ductility of TWIP steels is due to the formation of preferentially localised twins, which lead to extensive local strain hardening. Further twinning results in an increase in the volume fraction of twins leading to a marked decrease in the mean free path for dislocation movement. This results in the characteristic high levels of hardening in the material. These properties mean that TWIP steels are able to meet the requirements of high formability and energy absorption.

Although research into TWIP steels is increasing, the evolution of microstructure and grain statistics, such as elastic lattice strain and texture, especially during deformation have not been investigated in detail. Therefore limited information is available within this area. Microstructure and texture evolution during deformation have been investigated by few authors [13–15], however this has been achieved using *ex situ* interrupted testing and multiple samples. Consequently, the characterisation of the twins and texture has taken place after testing and only limited bulk information could be determined. Yan et al. [16] have used *in situ* synchrotron diffraction to characterise the interaction between slip and twinning during uniaxial tension. It was determined that the deformation texture is predominantly developed by dislocation gliding and that twinning impedes the reinforcement of texture.

Eshelby's [17,18] self consistent approach has successfully been used to simulate the uniaxial deformation texture and lattice strain behaviour of several materials [19–22]. However, the application of self-consistent modelling to TWIP steels has been rather limited. Prakash et al. [23] have utilised the visco-plastic self-consistent (VPSC) model framework to evaluate twin volume fraction and compare experimental and simulated deformation texture using two different twinning models. A predominant twin reorientation [24] model and the Kalidindi [25,26] approach were both evaluated, and the latter was found to predict more plausible twin activity and provide better agreement with experimentally observed textures. Experimental texture and grain statistics have also been modelled by Yan et al. [16] using both a VPSC and elasto-plastic self-consistent (EPSC) models. The VPSC model was utilised to simulate the experimental textures, but the model textures indicated an over prediction for the contribution of twinning in the simulation. Similarly the EPSC model was used to evaluate the experimental lattice strain evolution. However, the EPSC simulation did not include a twinning scheme, consequently the contribution of slip during deformation was only modelled for the lattice strain analysis.

In the present work, the texture evolution of a TWIP steel during tensile deformation has been investigated using *in situ* synchrotron X-ray diffraction. Lattice strain, peak width and intensity changes have also been examined, and the elasto-plastic self consistent model [20] has been utilised to rationalise the results. *Ex situ* microscopy and cyclic tensile loading experiments were also conducted, to augment the *in-situ* observations.

2. Experimental procedures

The TWIP steel tested (Fe–0.7C–2Al–15Mn–2Si wt%) was obtained in 3 mm rolled sheet form from Tata Steel Strip Mainland Europe. The stacking fault energy of the material was determined using thermodynamic calculations to be $31 \pm 10\ \mathrm{mJ\,m^{-2}}$ with adjustments made to account for the silicon and aluminium contents [27,28,5].

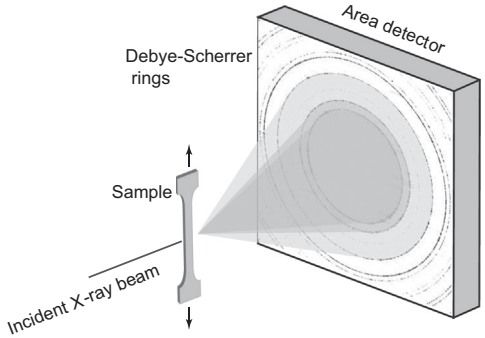

Fig. 1. Schematic representation of the experimental setup for *in situ* loading experiments. Fig. adapted from Ref. [29].

2.1. In situ synchrotron diffraction

In situ testing was carried out on beamline ID15B at the European Synchrotron Radiation Facility (ESRF), Grenoble, France. Tensile samples, with gauge dimensions of $19 \times 1.5 \times 1.5$ mm, were tested on an Instron 5 kN servohydraulic machine, with the tensile axis aligned to the rolling direction of the material. Samples were held in bespoke negative profile fixtures and loaded to an engineering strain of 22% in position control and at an initial strain rate of $10^{-3}\ \mathrm{s^{-1}}$ Full Debye–Scherrer diffraction rings were collected using a 300×400 μm monochromated X-ray beam of energy 67 KeV $\lambda = 0.1428$ Å on a Pixium 2D area detector located 1046 mm from the sample. A sampling time of 0.4 s was used. The experimental setup was identical to that used in Ref. [29] and testing was conducted consecutively, a schematic representation of the setup is shown in Fig. 1.

The texture during deformation was reconstructed by segmenting the diffraction rings into intensity-2θ profiles using 10° interval bins around the whole ring, using the program Fit2D [30]. Instrumental parameters were obtained by using a CeO_2 powder standard. The intensity-2θ profiles were then fitted through Rietveld refinement and the texture was plotted using an Extended-WIMV (E-WIMV)algorithm *via* the Materials Analysis Using Diffraction (MAUD) [31] program. Pole figures were visualised using the programs Pole8 and Pod2k.

Lattice strain is represented by the lattice spacings therefore the elastic strain in a certain direction for a peak {*hkl*} satisfying the diffraction condition can be determined by finding the lattice parameter d_i^{hkl} using Bragg's law, $\lambda = 2\mathrm{d}\,\sin\theta$ relative to an unstrained reference lattice parameter, d_0^{hkl}. Movement of the diffraction peaks can then be related to the elastic strain within grains in the diffraction orientation by

$$\epsilon_{hkl} = \frac{d_i^{hkl} - d_0^{hkl}}{d_0^{hkl}} \tag{1}$$

Therefore the shift of an {*hkl*} peak along the loading direction is a measure of strain in that {*hkl*} orientation.

To determine the lattice strains, individual diffraction peaks were fitted utilising a Gaussian function with the Wavemetrics program Igor Pro. *d*-spacing and intensity values for each peak were obtained from the 0 and 180° tensile loading bins.

2.2. Ex situ tensile testing

Ex situ tensile tests were carried out on a Zwick Roell 100 kN load frame and samples with gauge dimensions of $40 \times 8 \times 3$ mm